Gene Expression The Journal of Liver Research, Vol. 19, pp. 161–173
Printed in the USA.

1052-2166/19 $90.00 + .00
DOI: https://doi.org/10.3727/105221619X15529371970455
E-ISSN 1555-3884
www.cognizantcommunication.com

Sterol 12α-Hydroxylase Aggravates Dyslipidemia by Activating the Ceramide/mTORC1/SREBP-1C Pathway via FGF21 and FGF15

Preeti Pathak and John Y. L. Chiang

Department of Integrative Medical Sciences, Northeast Ohio Medical University, Rootstown, OH, USA

Sterol 12 -hydroxylase (CYP8B1) is required for the synthesis of cholic acid in the classic bile acid synthesis pathway and plays a role in dyslipidemia and insulin resistance. However, the mechanism of the involvement of Cyp8b1 in dyslipidemia and insulin resistance is not known. CYP8B1 mRNA and protein expression are elevated in diabetic and obese (*db/db*) mouse liver. In this study adenovirus-mediated transduction of CYP8B1 was used to study the effect of Cyp8b1 on lipid metabolism in mice. Results show that Ad-Cyp8b1 increased 12 -hydroxylated bile acids and induced sterol regulatory element-binding protein 1c (Srebp-1c)-mediated lipogenic gene expression. Interestingly, Ad-Cyp8b1 increased ceramide synthesis and activated hepatic mechanistic target of rapamycin complex 1 (mTORC1)-p70S6K signaling cascade and inhibited AKT/insulin signaling in mice. Ad-Cyp8b1 increased free fatty acid uptake into mouse primary hepatocytes. Ceramides stimulated S6K phosphorylation in both mouse and human primary hepatocytes. In high-fat diet-fed mice, Ad-Cyp8b1 reduced fibroblast growth factor 21 (FGF21), activated intestinal farnesoid X receptor (FXR) target gene expression, increased serum ceramides, VLDL secretion, and LDL cholesterol. In high-fat diet-induced obese (DIO) mice, Cyp8b1 ablation by adenovirus-mediated shRNA improved oral glucose tolerance, increased FGF21, and reduced liver triglycerides, inflammatory cytokine expression, nuclear localization of Srebp-1c and phosphorylation of S6K. In conclusion, this study unveiled a novel mechanism linking CYP8B1 to ceramide synthesis and mTORC1 signaling in dyslipidemia and insulin resistance, via intestinal FXR-mediated induction of FGF15 and liver FGF21. Reducing cholic acid synthesis may be a potential therapeutic strategy to treat dyslipidemia and nonalcoholic fatty liver disease.

Key words: Sterol 12α-hydroxylase (CYP8B1); Dyslipidemia; Insulin resistance; Ceramide/mTORC1/SREBP-1C pathway; Fibroblast growth factor 21 (FGF21); Fibroblast growth factor 15 (FGF15)

INTRODUCTION

Sterol 12 -hydroxylase (CYP8B1) is an enzyme required for the synthesis of cholic acid (CA) in the classic bile acid synthesis pathway, which is initiated by the rate-limiting enzyme cholesterol 7 -hydroxylase (Cyp7a1) to synthesize two primary bile acid chenodeoxycholic acid (CDCA) and CA in human liver[1]. In rodents, CDCA is converted to highly soluble -muricholic acid (-MCA) and -MCA, and 7 epimer, ursodeoxycholic acid (UDCA). CA has the lowest critical micellar concentration for solubilization of cholesterol and phospholipids to form mixed micelles, allowing for storage in the gallbladder, and is most efficient in the absorption of dietary cholesterol and fats into the intestine[2]. Bile acids are physiological agents that aid in the absorption of dietary lipids and steroids, xenobiotics and drugs for distribution, metabolism, and excretion. Bile acids also are signaling molecules that activate nuclear farnesoid X receptor (FXR) and Takeda G protein-coupled receptor 5 (TGR5) to maintain glucose, lipid, and energy homeostasis and to protect against inflammation in the liver and intestine[3]. Bile acids are conjugated to taurine or glycine for secretion into bile. In the intestine, conjugated CA and CDCA are deconjugated by gut bacterial bile salt hydrolase, and then bacterial 7 -dehydroxylase removes a 7 -hydroxyl group to form deoxycholic acid (DCA) and lithocholic acid (LCA), respectively[4]. About 95% of bile acids are reabsorbed in the ileum and circulated back to the liver via portal blood to inhibit bile acid synthesis. Bile acid hydrophobicity follows the order of LCA>DCA>CDCA>CA>UDCA> -MCA> -MCA. FXR expression is specific, mainly expressed in the gastrointestinal system[5], while TGR5 is expressed in most tissues including liver, intestine,

Address correspondence to John Y. L. Chiang, Ph.D., Department of Integrative Medical Sciences, College of Medicine, Northeast Ohio Medical University, 4209 SR 44, Rootstown, OH 44272, USA. Tel: 330-325-6694; Fax: 330-325-5910; E-mail: jchiang@neomed.edu

gallbladder, macrophages, and adipose tissues. In the liver, TGR5 is expressed in the sinusoidal endothelial cell (SEC), Kupffer cells (hepatic resident macrophages), stellate cells, and biliary epithelial cells in bile ducts, but not in hepatocytes[6,7]. Among bile acids, CDCA is the most potent endogenous ligand of FXR, while secondary bile acids, LCA and DCA, activate TGR5. The transcription of *Cyp7a1* and *Cyp8b1* genes is inhibited by FXR-induced small heterodimer partner (Shp) in the liver[8]. The gut to the liver axis plays a key role in regulating bile acid synthesis. Intestinal FXR induces fibroblast growth factor 15 (FGF15 or human FGF19) to activate hepatic FGF receptor 4/ERK signaling to inhibit *Cyp7a1* and *Cyp8b1* gene transcription[1]. *Cyp7a1* and *Cyp8b1* expression exhibits opposing diurnal rhythms, and fasting induces *Cyp8b1* but suppresses *Cyp7a1* expression, whereas feeding suppresses *Cyp8b1* but induces *Cyp7a1* expression[9]. This opposite effect of nutrient regulation of these two important regulatory genes in bile acid synthesis during fasting and refeeding cycle may determine bile acid composition and pool size to affect hepatic lipid and glucose metabolism.

Bile acid signaling through FXR and TGR5 plays a critical role in maintaining metabolic homeostasis and preventing metabolic diseases such as nonalcoholic fatty liver disease (NAFLD), which encompasses the simple steatosis, nonalcoholic steatohepatitis (NASH), fibrosis, and cirrhosis[10]. NAFLD is a major health problem worldwide and is associated with obesity and insulin resistance. It has been reported that type 2 diabetic patients have elevated serum 12 -hydroxylated bile acids (CA + DCA) and may be linked to insulin resistance[11]. Serum taurocholic acid (TCA) was elevated in human NAFLD patients[12]. It is not clear whether increased serum TCA is a cause or a consequence of NAFLD. Recently, the mechanistic target of rapamycin complex 1 (mTORC1) and its downstream target, ribosomal protein S6 kinase (S6K), have been linked to nutrient overloading-induced insulin resistance[13]. Several recent studies reported that deficiency of the *Cyp8b1* gene alleviates NAFLD and high-fat diet (HFD)-induced obesity (DIO)[14,15]. However, the underlying mechanism of the involvement of Cyp8b1 in dyslipidemia and NAFLD is not known and requires further study. To study the role of Cyp8b1 in dyslipidemia and insulin resistance, we used adenovirus-mediated overexpression of Cyp8b1 in wild-type and HFD-fed mice and silencing of Cyp8b1 in DIO mice. Our results showed that overexpression of Cyp8b1 induced intestinal FGF15 and increased ceramide synthesis, activated mTORC1 and S6K signaling to stimulate expression and maturation of steroid regulatory element-binding protein 1c (SREBP-1c), and hepatic lipogenesis in HFD-fed mice. Silencing of the *Cyp8b1* gene in DIO mice reduced FGF21, inactivated mTORC1/S6K singaling, and increased glucose tolerance and improved dyslipidemia. This study unveiled a novel mechanism linking Cyp8b1 to ceramide synthesis, FGF21, and mTORC1 signaling and dyslipidemia.

MATERIALS AND METHODS

Mice

Male C57BL/6J mice and leptin receptor-deficient obese *Lepr$^{db/db}$ (db/db)* male mice, 6–8 weeks of age, were purchased from Jackson Laboratory (Bar Harbor, ME, USA). Mice were fed a standard chow diet or a high-fat diet (HFD; 60% calories from fat; Research Diets, D12492) for 2 weeks as a nutrient overload and hepatic steatosis model or were fed a HFD for 4 months to develop obesity as a DIO mouse model. Mice were housed in a room with a 12-h light/dark cycle. The Institutional Animal Care and Use Committee of Northeast Ohio Medical University approved all animal protocols used in this study. To overexpress Cyp8b1, wild-type mice and HFD-fed male mice were injected via the tail vein with Ad-Cyp8b1 (Vector Bio Lab, Malvern, PA, USA) or Ad-GFP (Ad-Control) at 1×10^9 plaque-forming units per mouse and were killed 14 days later. To knock down the *Cyp8b1* gene, DIO mice were injected with adenovirus-shCyp8b1 (Ad-shCyp8b1) or Ad-shLacZ (Ad-shControl) and were killed 7 days later. All mice were fasted overnight and killed at 9 am. To study the mTORC1 signaling pathway, Ad-Cyp8b1 and Ad-GFP were injected in chow-fed mice, and 14 days later mice were fasted overnight. Male mice were intraperitoneally injected with mTORC1 inhibitor rapamycin (RAP; 2 mg/kg in saline buffer), extracellular signal-regulated kinase 1/2 (ERK1/2) inhibitor U0126 (2 mg/kg in 0.2% DMSO), or vehicle (0.2% PBS). Mice were sacrificed after 4 h, and liver mTORC1 and ERK signaling were monitored by immunoblot.

Cloning of Ad-shCyp8b1

Cyp8b1 shRNA was designed against sequences in Cyp8b1 exon-1: 5 -ACCGGTGTGAAGATGGCCTCT TTCCGAAGAAAGAGGCCATCTTCACACC-3 5 -AAAAGGTGTGAAGATGGCCTCTTTCTTCGG AAAGAGGCCATCTTCACACC-3 . The shRNA oligo sequence was cloned in pAd/CMV/V5-DEST vector (ThermoFisher, Waltham, MA, USA) as Ad-shCyp8b1 for knockdown of Cyp8b1. The scrambled shRNA oligo sequence was designed using BLOCK-it™ RNAi Designer (Invitrogen) and cloned in Ad-LacZ plasmid as Ad-shLacZ (Ad-shControl). Adenovirus was packaged in HEK293A cells. Low-titer viral stock was amplified and purified using the $CsCl_2$ gradient as reported previously[16].

Bile Acid Analysis

Bile acids in the liver, intestine (whole with its content), and gallbladder were extracted in 95% EtOH overnight,

in 80% EtOH for 2 h, and methanol/chloroform (2:1) for 2 h at 50°C. Bile acids were quantified using Bile Acid Assay kit (Genzyme Diagnostic, Framingham, MA, USA). Bile acid composition was analyzed by ultra-high-performance liquid chromatography/quadruple time-of-flight mass spectrometry as reported previously[17].

RNA Isolation and Quantitative Real-Time PCR (qPCR) Analysis

Total RNA was isolated with TRIzol reagent (Thermo Fisher). Reverse transcription reactions and real-time PCR were performed as described previously[16]. All primers/probe sets for qPCR were ordered from TaqMan Gene Expression Assays (Applied Biosystems, Foster City, CA, USA). Amplification of glyceraldehyde-3-phosphate dehydrogenase (Gaphd) was used as an internal control. Relative mRNA expression was quantified using the comparative CT (Ct) method and is expressed as $2^{-\Delta\Delta Ct}$.

Immunoblotting Analysis

Liver tissues were homogenized in RIPA buffer containing a cocktail of protease and phosphatase inhibitors (Cell Signaling Technology, Danvers, MA, USA). The protein content was determined by a BCA™ protein assay kit (Pierce, Rockford, IL, USA). The protein lysates were separated by 10% SDS-PAGE and transferred onto a polyvinylidene difluoride membrane (Millipore, Billerica, MA, USA). After blocking with 5% nonfat milk for 1 h at room temperature, the membrane was incubated with primary antibody overnight. Antibodies against Cyp8b1 (ab191910), Cyp7a1 (ab65596), and Cyp7b1 (ab138497) were purchased from Abcam (Cambridge, MA, USA). Antibodies against pAKT (#9271), AKT (#9272), S6K (#9205), pS6K (#9202), ERK (#9102), and pERK (#9101) were purchased from Cell Signaling (Danvers, MA, USA), and Srebp-1c antibody (NB100-60545) was from Novus Biologicals (Littleton, CA, USA).

H&E Staining

Mouse liver tissue was fixed in 4% paraformaldehyde for 48 h followed by paraffin embedding. Liver sections were stained with H&E and visualized under 40× magnification using a Olympus BX40 microscope.

Quantification of Tissue and Plasma Lipids

The liver was homogenized in PBS, and lipids were extracted in a mixture of chloroform and methanol (2:1), dried, and dissolved in 5% Triton X-100 in isopropanol. Hepatic and serum triglyceride and cholesterol levels were then quantified using Infinity reagents (ThermoFisher). Hepatic total free cholesterol was quantified using a kit from BioVision (Milpitas, CA, USA). Hepatic and plasma free fatty acid was quantified using a commercial kit (Wako, Osaka, Japan). Serum ceramides were analyzed as described previously[18].

Oral Glucose and Insulin Tolerance Tests

For the oral glucose tolerance test, DIO mice were injected with Ad-shCyp8b1 or Ad-shLacZ (Ad-shControl), and 7 days later mice were fasted 6 h and were orally gavaged with glucose (2 g/kg). Blood samples were collected via tail vein, and serum glucose was measured over 2 h using a OneTouch Ultra Mini glucometer (LifeScan, Milpitas, CA, USA).

Serum FGF21

Animals were fasted 6 h before collection of serum. Serum FGF21 level was measured using rat/mouse FGF21 Elisa assay kit (EZRMFGF21-26, Millipore, Burlington, MA, USA) according to the manufacturer's protocol.

VLDL Secretion Assay

Male C57BL/6J mice were injected with Ad-Cyp8b1 ($n = 5$) and Ad-GFP ($n = 5$) and were fasted for 6 h. Mice were injected with tyloxapol using tail vein injection. Retro-orbital blood collection was performed every hour, and serum triglycerides were measured.

Fast Protein Liquid Chromatography (FPLC) Analysis of Serum Lipoprotein Profiles

Male C57BL/6J mice were injected with Ad-Cyp8b1 ($n = 5$) and Ad-Control ($n = 5$). Two weeks later mice were fasted for 6 h before collecting sera. Sera were pooled from five mice. Serum sample (200 µl) was injected into a BioLogic DuoFlow QuadTec 10 system (Bio-Rad, Hercules, CA, USA) with a Superose 6 10/300 GL column (GE Healthcare), and a mobile phase buffer (0.15 mM NaCl, 0.01 M Na_2HPO_4, 0.1 mM EDTA, pH 7.5) was used to separate serum lipoproteins. The column fractions (0.5 ml each) were collected and assayed for cholesterol and triglycerides using an assay kit from ThermoFisher according to the manufacturer's protocol.

Free Fatty Acid Uptake Assay

Mouse primary hepatocytes were isolated and plated in a 48-well plate (6×10^4 cells in each well). Cells were then serum deprived for 1 h before treatment with QBT Fatty Acid Uptake solution (BODIPY-fatty acid + Q-Red.1 quencher in HBSS solution). Fluorescence emissions were recorded immediately with a Synergy-4 fluorescence plate reader (BioTek, Winooski, VT, USA) at 37°C. Instrument settings were as follows: bottom read, medium sensitivity, excitation 488/emission 515, with a filter cutoff at 495 nm[19]. The slope of fluoresce unit versus time was calculated. Slopes were represented (fatty acid uptake/min) with different concentrations of fatty acids added for uptake assay. Primary human hepatocytes

were obtained from the Liver Tissue and Cell Distribution System at the University of Pittsburgh.

Statistical Analysis

All experimental data are presented as mean ± standard error (SE). Statistical analysis was performed by Student's *t*-test. A value of $p < 0.05$ was considered a statistically significant difference.

RESULTS

CYP8B1 Expression Is Upregulated in Diabetes

Real-time PCR assay indicated that hepatic *Cyp8b1* mRNA expression increased threefold, while *Cyp7a1* increased twofold in leptin receptor-deficient $Lepr^{db/db}$ (*db/db*) mice compared to the wild-type mice (Fig. 1A, left). *Cyp7b1* mRNA of the alternative bile acid synthesis pathway was induced significantly. Immunoblotting showed that hepatic Cyp8b1 and Cyp7b1 protein expression was elevated in *db/db* mice compared to wild-type mice, while there was no change in Cyp7a1 protein expression (Fig. 1A, right). Liver lipogenic genes fatty acid synthase (*Fas*) and stearoyl-CoA desaturase 1 (*Scd1*), and their transcriptional activator *Srebp-1c* mRNA levels were significantly increased in *db/db* mice compared to wild-type mice (Fig. 1B). However, expression of FXR-induced gene *Shp* was not altered in *db*/*db* mice, indicating that hepatic FXR was not activated in *db/db* mice (Fig. 1B). In the intestine, FXR target genes including organic solute transporter β (*Ostβ*) and *Shp* mRNA expression levels were increased in *db/db* mice compared to wild-type mice (Fig. 1C). These results indicate that bile acid synthesis is dysregulated, and SREBP-1c-mediated lipogenesis is stimulated in *db/db* mice.

Adenovirus-Mediated Overexpression of Cyp8b1 Increased Hepatic Lipogenic Gene Expression and Free Fatty Acid Uptake

To test the effect of Cyp8b1 on hepatic metabolism, hemagglutinin tagged (HA)-Cyp8b1 adenovirus (Ad-Cyp8b1) was administrated to the chow-fed mice. Adenovirus overexpression increased *Cyp8b1* mRNA expression by sevenfold compared to Adeno-Gfp (Ad-Control)-injected mice (Fig. 2A, left) and significantly increased Cyp8b1 protein levels (Fig. 2A, left inset). Ad-Cyp8b1 did not alter the expression of other bile acid synthesis genes including *Cyp7a1*, *Cyp27a1*, *Cyp7b1*, and aldoketoreductase 1D1 (*Akr1d1*) mRNA expression (Fig. 2, middle). Interestingly, Ad-Cyp8b1 induced expression of lipogenic genes *Srep-1c* and *Fas* mRNA, but reduced *Srebp-2* expression and had no effect on *Shp* or *Scd1* mRNA expression (Fig. 2A, right). However, Ad-Cyp8b1 did not alter serum or liver cholesterol or triglyceride levels (data not shown). As expected, Ad-Cyp8b1 altered the gallbladder bile acid composition by markedly increasing TCA, CA, and TDCA, and reducing T- -MCA and -MCA (Fig. 2B). Increasing Cyp8b1 expression did not increase bile acid pool size (bile acid content in liver, intestine, and gallbladder) compared to Ad-Control mice (Fig. 2C). Ad-Cyp8b1 significantly increased mRNA expression of liver-specific fatty acid-binding protein *Fabp-1, Fabp-2,* and *Fabp-5*, but not *Fabp6* or *Cd36* or the sphingosine-1-phosphate receptor 2 (S1pr2) (Fig. 2D). Fatty acid uptake assay showed rapid uptake of palmitate into mouse primary hepatocytes isolated from mice infected with Ad-Cyp8b1 compared to Ad-control hepatocytes (Fig. 2E). However, Ad-Cyp8b1 did not increase liver inflammatory gene tumor necrosis factor (Tnf), cyclin D14 (Cd14), interleukin-6 (IL-6), interferon- (Inf), INF -induced protein-10 (Ip-10), or Il-18 mRNA expression, or serum AST or ALT levels (Fig. 2F). Ad-Cyp8b1 induced ileum *Fxr*, *Shp*, and *Fgf15* mRNA expression indicating activation of intestinal FXR activity. Overall, these results indicate that increasing Cyp8b1 expression stimulates lipogenesis, increases TCA and TDCA, increases free fatty acid uptake into mouse hepatocytes, and activates intestinal FXR activity.

Ad-Cyp8b1 and Ceramides Stimulate mTORC1/S6K Signaling in Chow-Fed Mice

Activation of the mechanistic target of rapamycin complex 1 (mTORC1) pathway has been linked to activation of Srebp-1c processing[20] and increase of free fatty acid uptake[21,22]. Therefore, we wanted to investigate whether Ad-Cyp8b1 activates the mTORC1 pathway by stimulating phosphorylation of its downstream target S6K. Ad-Cyp8b1 mice were fasted overnight and fed chow diet for 4 h, with or without intraperitoneal injection of the mTORC1 inhibitor rapamycin (RAP) and the ERK1/2 inhibitor (U0126). Figure 3A shows that Ad-Cyp8b1 increased S6K phosphorylation (pS6K), which was suppressed by RAP but not U0126. In contrast, Ad-Cyp8b1 reduced phosphorylation of AKT (pAKT) in insulin signaling, which was prevented by RAP. These data are consistent with activation of the mTORC1 pathway antagonizing insulin signaling in hepatocytes[23]. Increased phosphorylation of S6K correlates with the increase in the nuclear form of Srebp-1c (nSrebp-1c) in Ad-Cyp8b1 mice (Fig. 3A). We assayed ERK1/2 phosphorylation in Ad-Cyp8b1 mice. Figure 3A shows that Ad-Cyp8b1 induced ERK phosphorylation, which was inhibited by RAP (Fig. 3A). These results suggest that Cyp8b1 activates mTORC1 via activation of ERK1/2 signaling. Ceramides are known to activate mTORC1 signaling[24]. Ad-Cyp8b1 induced liver ceramide synthase 2 (*CerS2*), the rate-limiting enzyme in ceramide synthesis, but not serine palmitoyltransferase long-chain base

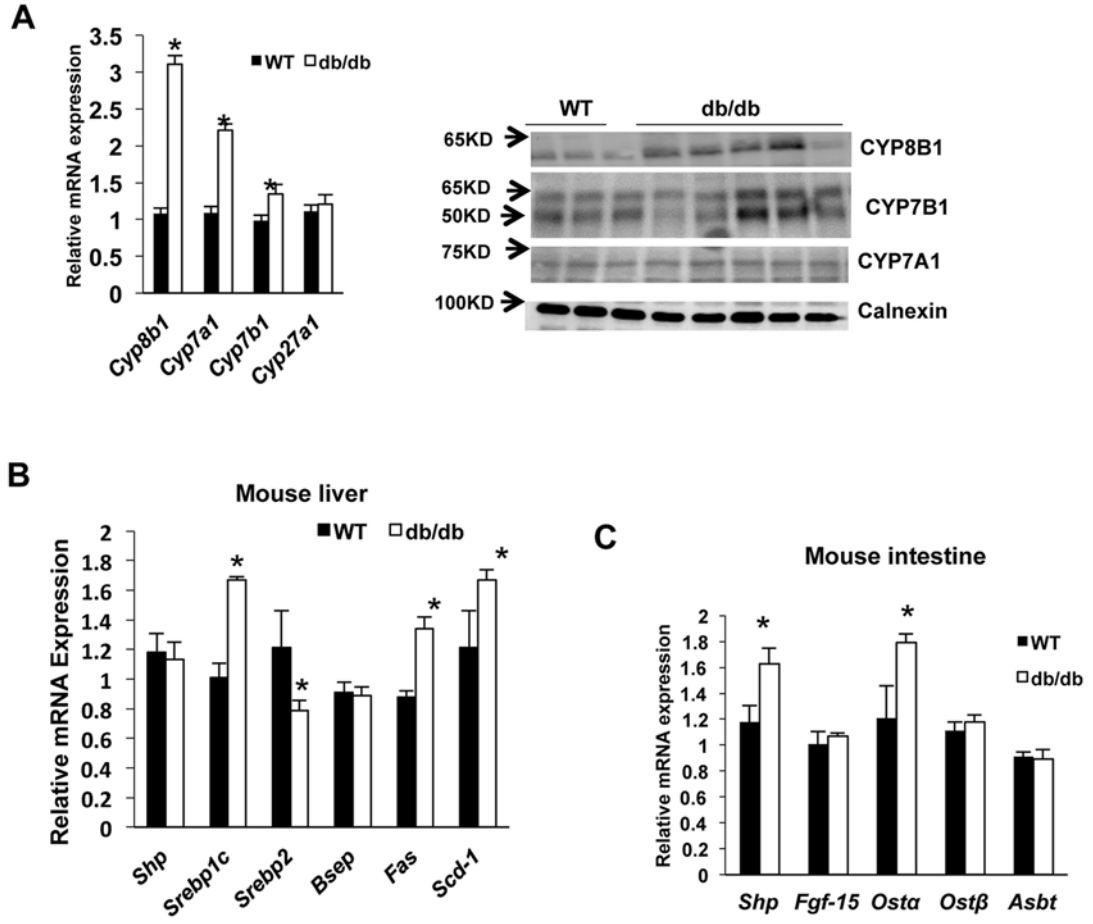

Figure 1. Sterol 12 -hydroxylase (Cyp8b1) expression in diabetic and obese (*db/db*) mice. Wild-type C57BL/6J mice ($n=6$) and *db/db* mice ($n=5$) were sacrificed after 6 h of fasting. (A) Real-time PCR (qPCR) analysis of liver bile acid synthesis gene mRNA expression (left). Immunoblot of liver microsomal Cyp7a1, Cyp8b1, and Cyp7b1 protein expression in wild-type ($n=3$) and *db/db* mouse liver ($n=5$) (right). Calnexin was used as an internal control for microsomal proteins. (B) Mouse liver farnesoid X receptor (FXR) target gene mRNA expression in wild type and *db/db* mice. (C) Mouse intestine FXR target gene mRNA expression. Relative mRNA expression was calculated with respect to normal liver samples compared to human steatosis. Results are shown as means ± SE. *S*tudent's *t*-test was used for statistical analysis. *Statistically significant difference ($p<0.05$), WT versus *db/db* mice.

subunit 1 (*Sptlc1*) and *Sptlc2*, nor Delta 4-desaturase sphingolipid-1 (*Degs-1*) mRNA expression (Fig. 3B, right). In the ileum, both *CerS2* and *Sptlc2* were significantly upregulated (Fig. 3B, right). We then studied the effect of ceramides on S6K phosphorylation in mouse and human primary hepatocytes. Treatment with ceramides 16:0 and 18:0 increased phosphorylation of S6K in mouse and human primary hepatocytes (Fig. 3C). Ceramide treatment had a reduced effect on ERK1/2 phosphorylation in mouse primary hepatocytes and had no effect on ERK1/2 phosphorylation in human primary hepatocytes. Overall these results indicate that overexpression of Cyp8b1 stimulates mTORC1-S6K signaling and SREBP-1c maturation, but inhibited insulin/AKT signaling. These results suggest that Cyp8b1 stimulation of mTORC-S6K signaling and nSREBP-1c may be mediated by ceramides in hepatocytes.

Ad-Cyp8b1 Induced Lipogenesis, mTORC1 Signaling, and Ceramide Synthesis in Short-Term High-Fat Diet-Fed Mice

We next studied the effect of Ad-Cyp8b1 on mTORC1 signaling in short-term high-fat diet (HFD)-fed mice as a model of nutrient overload. Mice were injected with Ad-Cyp8b1 and fed HFD for 2 weeks. There was no significant change in body weight and food intake in Ad-Cyp8b1 mice compared to Ad-Control injected mice (Fig. 4A). Interestingly, Ad-Cyp8b1 improved insulin tolerance, while there was no change in glucose

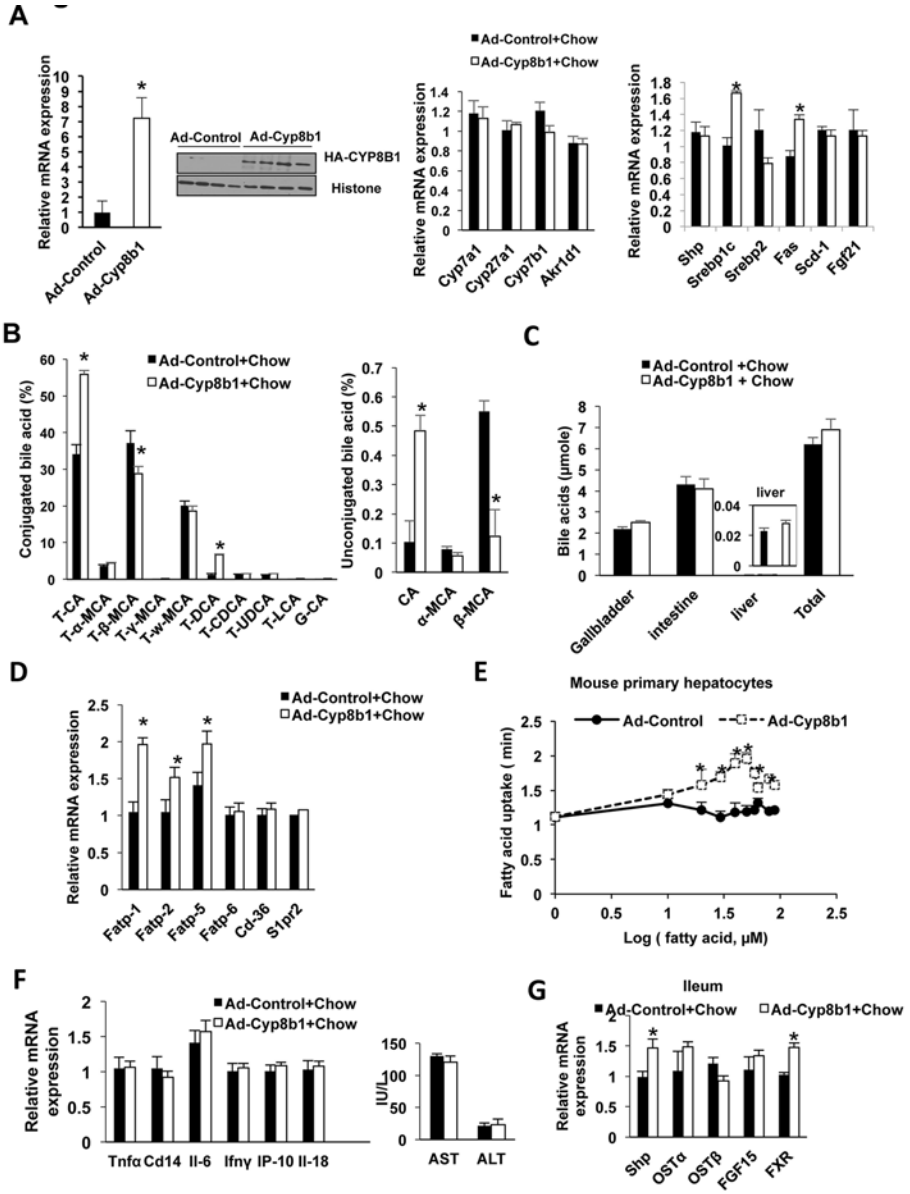

Figure 2. Metabolic analysis of mice transduced with Ad-CYP8B1. Wild-type C57BL/6J mice were injected with Ad-Cyp8b1 (Ad-cyp8b1, $n = 8$) or Ad-Control ($n = 8$) for 2 weeks. Mice were fasted for 6 h and sacrificed. (A) Expression of bile acid synthesis genes in mouse liver. Left: qPCR analysis of liver *Cyp8b1* mRNA expression. The inset shows immunoblot of HA-CYP8B1 in liver extracts. Middle: qPCR analysis of liver bile acid synthesis gene mRNA expression. Right: qPCR analysis of mRNA expression of liver lipogenic genes *Srebp-1c*, *Srebp-2*, fatty acid synthase (*Fas*), and stearoyl-CoA desaturase 1 (*Scd1*), fibroblast growth factor 21 (FGF21) mRNA expression. (B) Bile acid composition analysis of gallbladder bile. (C) Total bile acid pool size (bile acids in gallbladder liver and intestine). (D) qPCR analysis of liver fatty acid transport proteins (*FATPs*) and *Cd-36* mRNA expression. (E) Free fatty acid uptake assay. Mouse primary hepatocytes were treated with palmitate, and fatty acid uptake rates were assayed using BODIPY. (F) qPCR analysis of liver inflammatory cytokine mRNA expression (left), and serum AST and ALT levels (right). (G) qPCR analysis of expression of FXR target gene mRNA in the ileum of Ad-Cyp8b1 mice. Results shown are means ± SE. Student's *t*-test was used for statistical analysis. *$p < 0.05$, versus chow mice injected with Ad-GFP. *Statistically significant difference ($p < 0.05$), Ad-CYP8B1 versus Ad-control mice.

tolerance compared to Ad-Control injected mice (Fig. 4B). Ad-Cyp8b1 significantly increased liver triglycerides but not serum cholesterol or triglycerides, nor serum AST or ALT levels in HFD-fed mice (Fig. 4C). However, Ad-Cyp8b1 significantly reduced serum FGF21 in HFD-fed mice (Fig. 4D). H&E staining shows that HFD caused hepatic steatosis, and Ad-Cyp8b1 increased hepatic steatosis in HFD-fed mice (Fig. 4E).

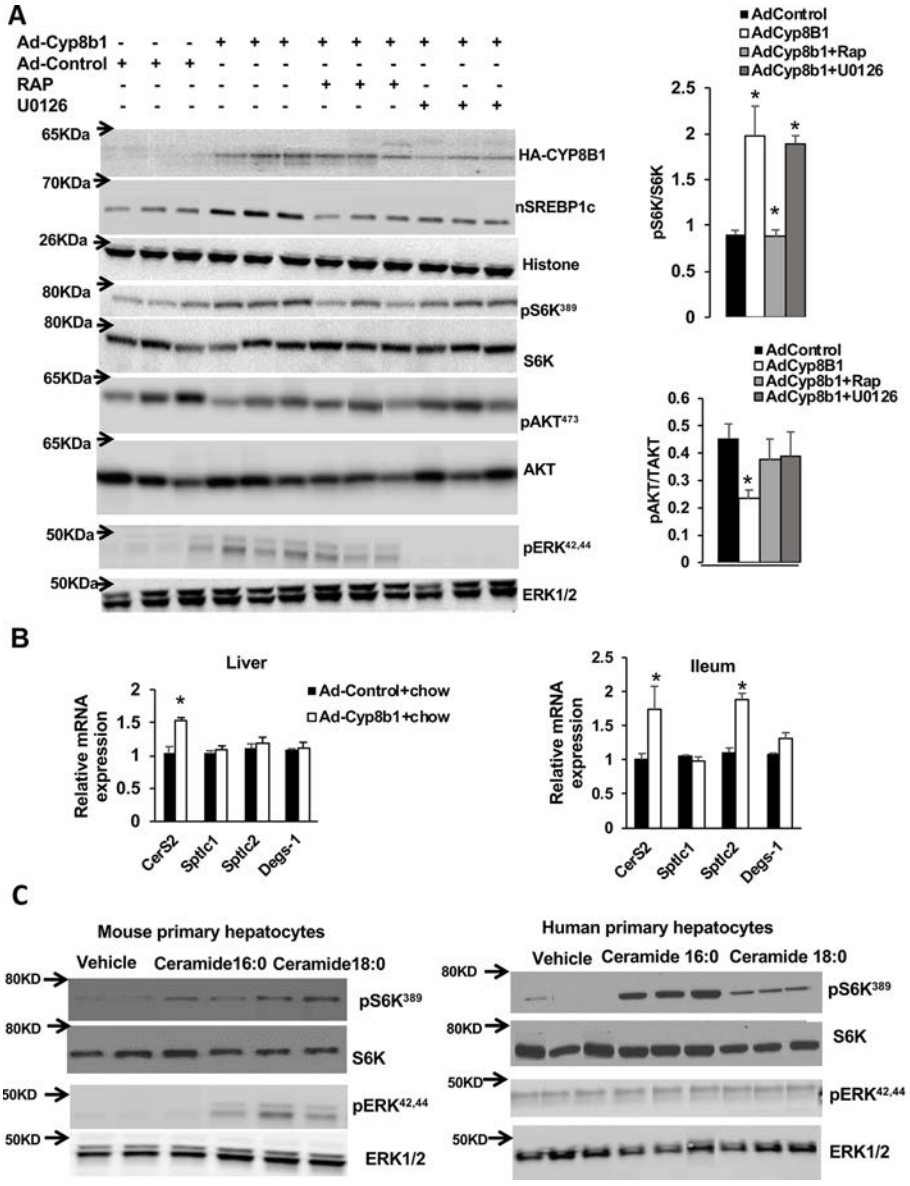

Figure 3. Effect of Ad-Cyp8b1 on hepatic mechanistic target of rapamycin complex 1 (mTORC1) signaling in mice. Wild-type C57BL/6J mice were injected with Ad-Cyp8b1 ($n = 5$) or Ad-Control ($n = 5$). Overnight fasted mice were fed chow diet for 4 h and were IP injected with the mTORC1 inhibitor rapamycin (RAP; 0.5 mg/kg), the ERK1/2 inhibitor U0126 (0.5 mg/kg), or vehicle (0.2% DMSO) for 1 h and were sacrificed. (A) Immunoblot analysis of HA-CYP8B1, nuclear SREBP-1c (nSREBP-1c), total S6K and AKT, ERK1/2 and phosphorylated S6K (pS6K), phosphorylated AKT (pAKT), and phosphorylated-ERK. Liver nuclear extracts were used for the assay of nSREBP-1c and histone as the internal control. Liver cytoplasmic protein extracts were used for assay phosphorylation of S6K, AKT, and ERK. (B) qPCR analysis of ceramide synthesis gene mRNA expression. (C) Immunoblot analysis of phosphorylation of S6K and ERK1/2 in mouse primary hepatocytes (left) and human primary hepatocytes (right). pERK1/2 is phosphorylated ERK1/2. Human and mouse primary hepatocytes were treated with 30 mM each of C16:0 or 18:0 ceramide indicated for 2 h. Each lane represents one primary hepatocyte preparation isolated from mouse liver or human donor liver. Student's *t*-test was used for statistical analysis. *Statistically significant difference ($p < 0.05$), Ad-CYP8B1 versus Ad-control mice.

FPLC analysis of serum lipids shows that LDL cholesterol (fractions Nos. 18–21) was increased in HFD-fed Ad-Cyp8b1 mice (Fig. 4F, top). Ad-Cyp8b1 did not affect triglycerides in the VLDL fractions (Nos. 10–14) but increased triglycerides in LDL fractions (Nos. 18–21) (Fig. 4F, bottom). Interestingly, Ad-Cyp8b1 significantly increased serum ceramide species, C16:00, C18:00, C22:0, and C24:0 in HFD-fed mice (Fig. 4G). Ad-Cyp8b1 increased VLDL secretion rate in HFD-fed mice compared to adenovirus control mice (Fig. 4H). Overall,

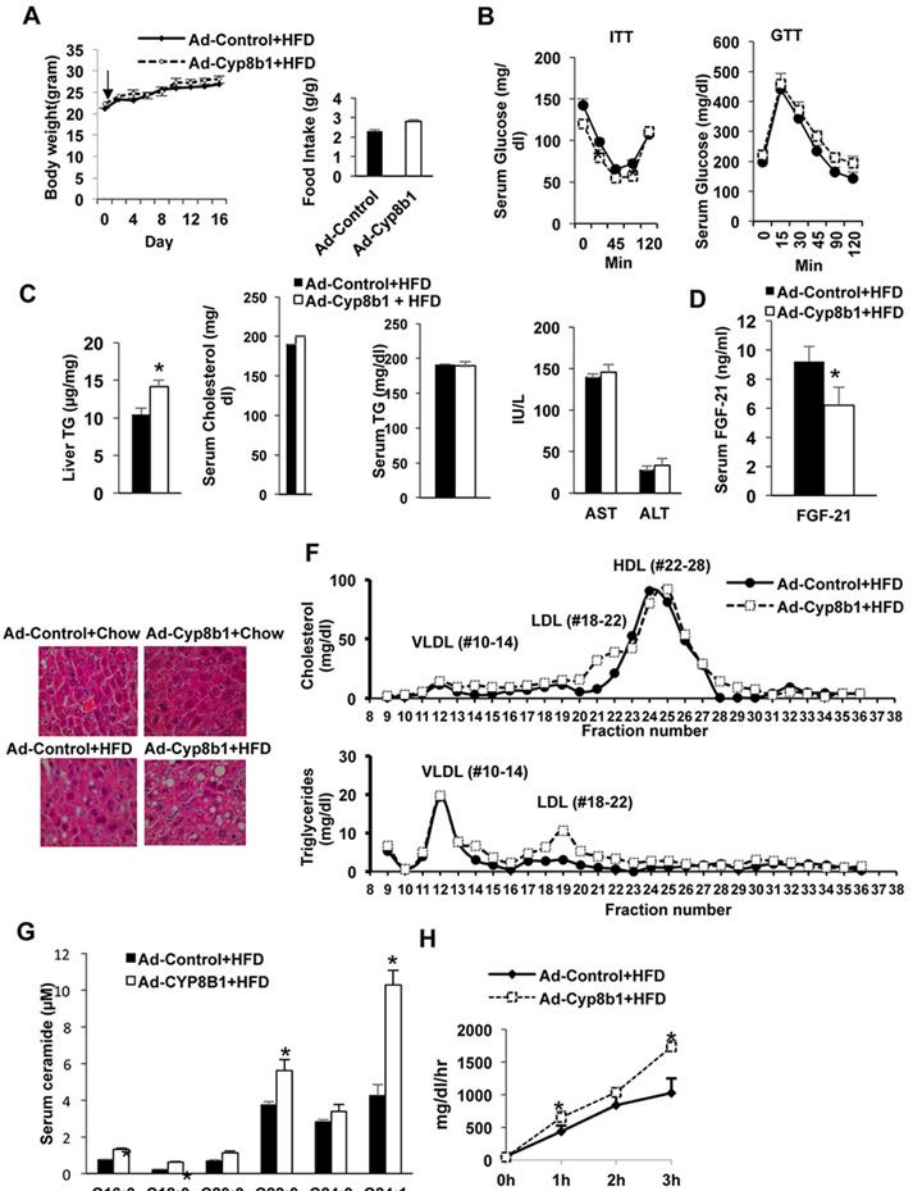

Figure 4. Effect of Ad-Cyp8b1 on lipid and lipoprotein metabolism in high-fat diet (HFD)-fed mice. Wild-type C57BL/6J mice were injected with Ad-CYP8B1 ($n = 11$) or Ad-Control ($n = 11$; indicated by an arrow). Mice were fed a high-fat diet (60% calorie from fat) for 2 weeks. Mice were fasted for 6 h before sacrifice. (A) Body and food intake of HFD-fed mice injected with Ad-CYP8B1 compared to Ad-Control HFD-fed mice. (B) Insulin tolerance test (ITT) and glucose tolerance test (GTT) of HFD-fed mice injected with Ad-Cyp8b1 compared to Ad-control HFD-fed mice. ITT was performed on the 11th day after adenovirus injection (left), and GTT was performed on the 13th day after adenovirus injection. (C) Liver triglyceride (TG); serum cholesterol and triglyceride; and serum AST and ALT. (D) Serum FGF21 protein levels. (E) H&E staining of lipids in livers of chow-fed and HFD-fed mice injected with Ad-Cyp8b1 or Ad-Control virus (representative image from one liver in each group). Representative images are shown. (F) FPLC analysis of serum cholesterol and triglyceride. Sera were pooled from five Ad-Cyp8b1 and five Ad-Control mice for analysis. Serum cholesterol (top) and serum triglycerides (bottom) were assayed in each FPLC fractions: VLDL (Nos. 10–14), LDL (Nos. 18–22), and HDL (Nos. 22–28). (G) Serum ceramides in Ad-Cyp8b1. (H) VLDL secretion assay. Results are shown as means ± SE. Student's *t*-test was used for statistical analysis. *Statistically significant difference ($p < 0.05$), Ad-Cyp8b1 versus Ad-Control mice.

Ad-Cyp8b1 combined with short-term HFD feeding significantly elevated VLDL secretion rate, serum ceramide, and LDL cholesterol, without increasing serum cholesterol, triglycerides, or inflammation markers.

We then fed mice with HFD and treated with Ad-Cyp8b1 or Ad-Control for 2 weeks to study the effect of overexpression of CYP8B1 on lipid metabolism. Figure 5A shows that Ad-Cyp8b1 increased

Cyp8b1 mRNA levels by seven- to eightfold, but did not change liver *Cyp7a1*, *Cyp7b1*, *Cyp27a1*, or *Akr1d1* mRNA expression in HFD-fed mice (Fig. 5A). Figure 5B shows that Ad-Cyp8b1 increased mRNA expression of liver lipogenic genes *Srebp-1c*, *Fas* and *Scd1*, reduced *Fgf21*, while it had no change in Shp, Srebp-2, and S1pr2 mRNA expression (Fig. 5B). Ad-Cyp8b1 induced liver mRNA expression of ceramide synthesis genes CerS2, *Sptlc1*, and *Degs-1*, and triglyceride synthesis genes diacylglycerol acyltransferase (*Dgat*) and glycerol-3-phosphate acyltransferase (*Gpat*) in HFD-fed mice (Fig. 5C). However, Ad-Cyp8b1 did not further increase nSREBP-1c protein and phosphorylation of S6K1, but reduced AKT phosphorylation in HFD-fed mice (Fig. 5D). In the ileum, Ad-Cyp8b1 activated intestinal FXR signaling by inducing *Shp*, *OSTa*, and *Fgf15* mRNA expression, and *CerS2* and *Sptlc1* mRNA (Fig. 5E). These results indicate that Ad-Cyp8b1 increased liver lipogenic gene expression, Srebp-1c maturation, intestinal ceramide synthesis, and mTOR-pS6K signaling in this short-term HFD-fed mouse model.

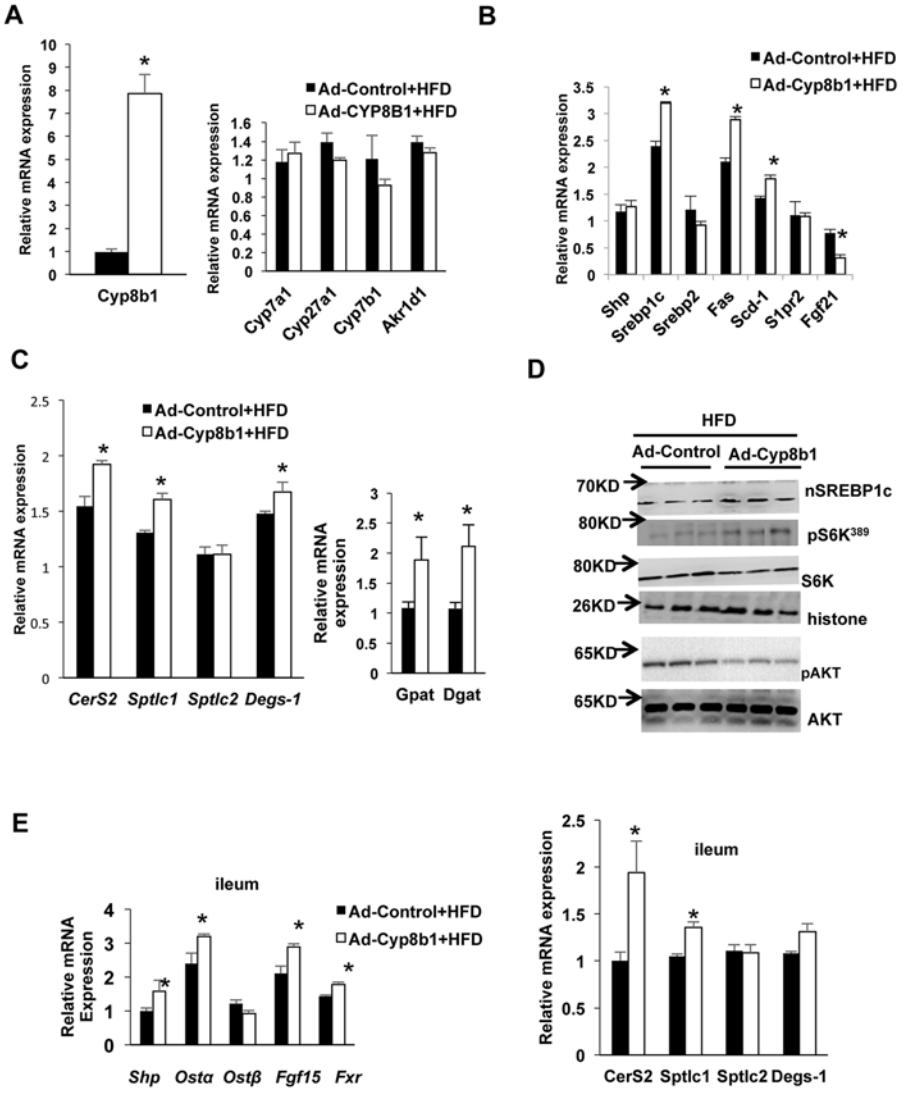

Figure 5. Effect of Ad-Cyp8b1 on liver and intestine gene expression and mTORC1 signaling in HFD-fed mice. Wild-type C57BL/6J mice were injected with Ad-CYP8b1 ($n = 11$) or Ad-GFP control ($n = 11$) and fed with high-fat diet (60% kcal from fat) for 2 weeks. Mice were fasted for 6 h before sacrifice. (A) qPCR analysis of bile acid synthesis gene mRNA expression. (B) qPCR analysis of liver lipogenic gene mRNA expression. (C) qPCR analysis of liver ceramide synthesis gene mRNA expression (left) and triglyceride synthesis gene mRNA expression (right). (D) Immunoblot analysis of nSREBP-1c and phosphorylation of S6K and AKT. (E) qPCR analysis of ileum FXR target gene and ceramide synthesis gene mRNA expression. Results shown are means ± SE. Student's *t*-test was used for statistical analysis. *Statistically significant difference ($p < 0.05$), Ad-Cyp8b1 versus Ad-Control mice.

Deletion of Cyp8b1 Improved Dyslipidemia in Diet-Induced Obese Mice

We then fed wild-type mice with HFD for 4 months to induce obesity in mice, and then Ad-shCyp8b1 (shCyp8b1) or Ad-shControl was transduced in DIO mice for 2 weeks to study the effect of silencing of Cyp8b1 expression on insulin sensitivity and dyslipidemia. There was no significant change in body weight, serum total cholesterol, and triglyceride of DIO mice injected with Ad-shCyp8b1 compared to Ad-shControl injection in 2 weeks (Fig. 6A, left). Oral glucose

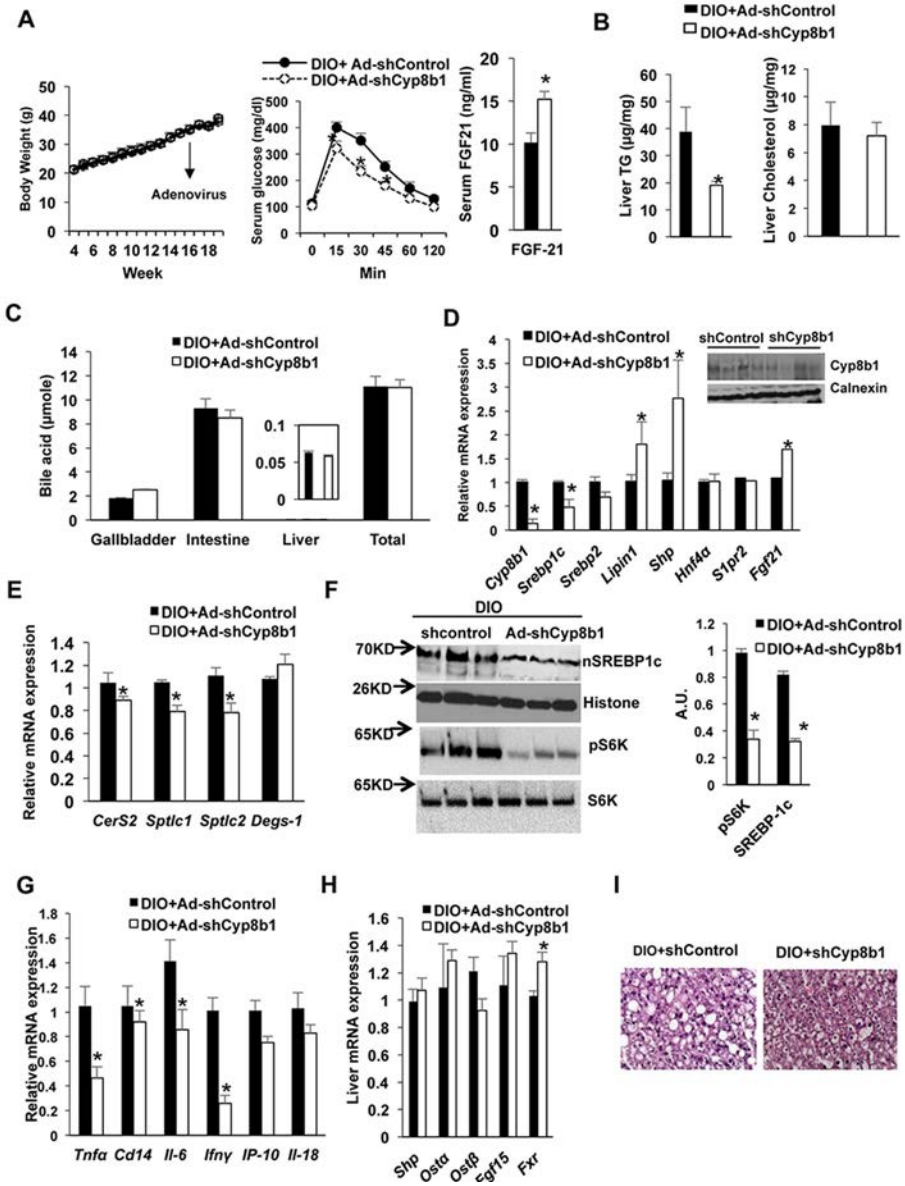

Figure 6. Effect of silencing Cyp8b1 in high-fat diet-induced obese (DIO) mice. Wild-type C57BL/6J mice were fed with HFD for 4 months. DIO mice were then injected with Ad-shCyp8b1 ($n = 10$) or Ad-shLacZ (Ad-shControl, $n = 8$) (indicated by an arrow) and were fasted for 6 h before sacrificed. (A) Body weight and glucose tolerance of Ad-shCYP8b1 DIO mice. Mice were fed HFD for 16 weeks. Ad-Cyp8b1 was injected to mice at time indicated by an arrow. Oral glucose tolerance test (left) and serum FGF21 levels (right). (B) Liver cholesterol and triglycerides. (C) Bile acid pool size. (D) qPCR analysis of liver Cyp8b1 and lipogenic gene mRNA expression. Immunoblot analysis shows that Ad-shCyp8b1 reduced Cyp8b1 protein levels in mouse livers ($n = 3$). (E) qPCR analysis of liver ceramide synthesis gene mRNA expression. (F) Immunoblot analysis of liver nSREBP-1c and phosphorylation of S6K. (G) qPCR analysis of liver inflammatory cytokine mRNA expression. (H) qPCR analysis of ileum FXR target gene mRNA expression. (I) Liver H&E staining of DIO + shControl and DIO + Cyp8b1 fed with high-fat diet for 4 months (representative of a liver each). Results are shown as means ± SE. Student's *t*-test was used for statistical analysis. *Statistically significant difference ($p < 0.05$), Ad-shCyp8b1 versus Ad-shControl.

tolerance test showed that Ad-shCyp8b1 improved glucose tolerance (Fig. 6A, right), increased serum FGF21 levels, and reduced liver triglycerides, whereas it had no effect on liver cholesterol in DIO mice (Fig. 6B). Ablation of Cyp8b1 did not change total bile acid pool size or distribution of bile acids in gallbladder, liver, and intestine compared to Ad-shControl mice (Fig. 6C). Ad-shCyp8b1 reduced *Cyp8b1* mRNA expression by 90% and reduced *Srebp-1c* and *Srebp-2* mRNA levels compared to Ad-shControl mice (Fig. 6D). Immunoblot analysis shows that Ad-shCyp8b1 reduced Cyp8b1 protein levels in mouse liver compared to Ad-shControl (Fig. 6D, inset). Interestingly, Ad-shCyp8b1 significantly increased *Shp* mRNA levels, indicating activation of liver FXR activity (Fig. 6D); Fgf21 and *lipin1* mRNA levels were also increased (Fig. 6D). Ad-shCyp8b1 reduced liver *CerS2*, *Sptlc1*, and *Sptlc2* mRNA levels compared to Ad-shControl mice (Fig. 6E). Ad-shCyp8b1 significantly reduced nSrebp-1c and S6K phosphorylation in DIO mice compared to Ad-shControl mice (Fig. 6F). Ad-shCyp8b1 also significantly reduced liver inflammatory markers, *Il-6*, *Ip-10*, *Tnfα*, and *Ifnγ* mRNA expression compared to Ad-shControl in DIO mice (Fig. 6G). However, Cyp8b1 deletion did not alter intestinal FXR target gene mRNA expression (Fig. 6H) or serum lipid profile in DIO mice (data not shown). H&E staining indicates that Ad-shCyp8b1 reduced lipid content in mouse livers (Fig. 6I). These results indicate that ablation of Cyp8b1 reduced liver ceramide synthesis, induced liver FGF21 production, and inhibited mTORC1/S6K1 signaling to improve glucose tolerance and reduce hepatic inflammation in DIO mice.

DISCUSSION

The aim of this study was to elucidate the mechanism of Cyp8b1 involvement in dyslipidemia and insulin resistance. Overexpression of Cyp8b1 increased TCA and TDCA, which may activate intestinal FXR. Intestinal FXR induces synthesis of ceramides, which activates hepatic mTORC1/S6K signaling and Srebp-1c-mediated lipogenesis (Fig. 7). The mTORC1/S6K pathway plays a critical role in inhibiting insulin signaling[13]. It has been reported that insulin stimulation of SREBP-1c processing to its nuclear form requires S6K, and deficiency of the liver-specific S6K protects against hepatic steatosis by reducing Srebp-1c expression and maturation, suggesting that mTORC1/S6K signaling plays an important role in the fasting/feeding response, hepatic steatosis, and insulin resistance[25,26]. Our current study uncovered a novel link involving Cyp8b1-mediated activation of the mTORC1/S6K/SREBP-1c pathway to cause dyslipidemia and insulin resistance.

This study also showed that Ad-Cyp8b1 decreased FGF21 expression in HFD-fed mice, whereas shCyp8b1

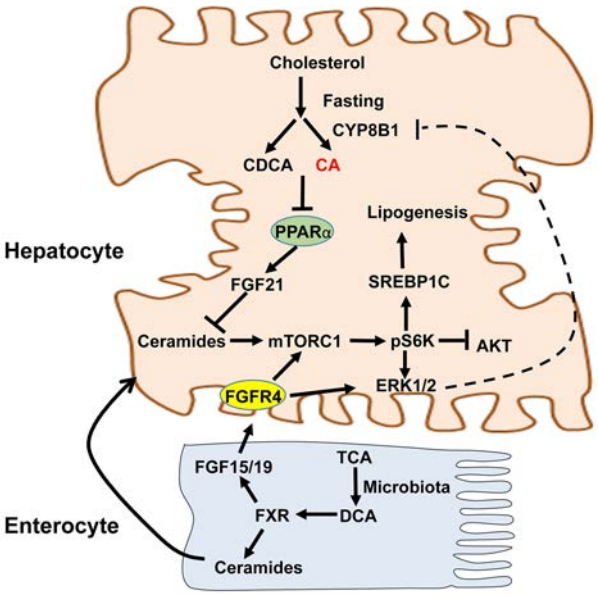

Figure 7. Mechanism of CYP8B1 activation of ceramide/mTOR/SREBP-1C signaling. CYP8B1 increases TCA, which is converted to DCA by gut microbiota. In the intestine, TDCA activates intestinal FXR to induce ceramides and FGF15 synthesis. CYP8b1 activates mTORC1 by two mechanisms. First, ceramides synthesized in enterocytes are secreted into blood circulation to activate the mTORC1-S6K pathway in hepatocytes to induce SREBP-1C-mediated hepatic lipogenesis. Second, TCA/TDCA induces intestinal FGF15 to activate hepatic FGFR4 to activate mTORC1. mTORC1 activates ERK1/2 signaling via pS6K. Activation of ERK1/2 may serve as a negative mechanism to inhibit CYP8B1. Therefore, CA and DCA modulate mTORC1 signaling and insulin signaling and lipogenesis in hepatocytes to maintain lipid homeostasis. Bile acids inhibit PPAR , which induces FGF21 as a fasting response. FGF21 inhibits mTORC1 through increased adiponectin secretion from adipose tissue and increase hepatic AKT/insulin sensitivity. CYP8B1 inhibits hepatic synthesis of FGF21, which inhibits mTORC1 signaling, and results in activation of mTORC1 signaling.

induced FGF21 expression in DIO mice. FGF21 has emerged as a fasting-induced hormone that mimics insulin action to regulate glucose and energy metabolism[27,28]. It has been reported that FGF21 reduces serum triglycerides by stimulating energy metabolism in adipose tissues[29] and rapidly increases adiponectin secretion from adipose tissue to reduce ceramides and stimulate energy metabolism in DIO mice[30]. Our previous study shows that bile acids inhibit transcription of peroxisome proliferator-activated receptor (PPAR)[31]. PPAR induces FGF21[27], which then inhibits mTORC1 (Fig. 7). Recent studies show that FGF21 inhibits mTORC1 signaling to improve insulin sensitivity and reduce hepatic steatosis in DIO mice[32,33]. Thus, increasing Cyp8b1 expression decreases FGF21 expression and stimulates mTORC1/ceramide

signaling to stimulate Srebp-1c-mediated lipogenesis. In addition, increased TCA and TDCA stimulates intestinal FXR/FGF15 signaling to stimulate mTORC1 via FGFR4 signaling (Fig. 7).

Interestingly, Ad-Cyp8b1 induced intestinal *Fgf15* expression and ceramide synthesis in HFD-fed mice. This effect was mainly through activation of intestinal FXR, which is known to induce ceramide synthesis and serum ceramide levels[18]. Ceramides cause ER stress and mitochondrial oxidative stress, contributing to NAFLD[34]. In hepatocytes, ceramides inhibit AKT and cause hepatic insulin resistance[35]. TCA is a very weak FXR agonist (EC_{50} = ~0.6 mM). In the colon, TCA is converted to DCA by gut bacteria. Ad-Cyp8b1 markedly increased TCA and TDCA to levels that could be high enough to activate intestinal FXR to induce ceramide synthesis in Ad-Cyp8b1 mice. High-fat diet is known to induce TCA to promote dysbiosis and contribute to liver inflammation[36]. TCA/DCA-induced dysbiosis may be through activation of intestinal FXR to increase ceramides. Robust increases in serum ceramide species may lead to stimulation of mTORC1-S6K signaling in hepatocytes. S6K can be activated by mTORC1 or ERK1/2[37]. A recent study showed that FGF19 activated mTORC1/pS6K and ERK1/2 in hepatoma cells[38]. We reported previously that FGF19 activates FGFR4/ERK1/2 signaling in human hepatocytes to inhibit CYP7A1 and CYP8B1 via ERK1/2 pathway[39]. Therefore, increasing TCA and TDCA activates mTORC1 signaling via two signaling mechanisms: FXR/ceramide and FXR/FGF15/FGFR4 pathways (Fig. 7). Figure 7 illustrates the role of CYP8B1 in stimulating lipogenesis via mTORC1, which is activated by FGF15/19/FGFR4/ERK1/2 and FXR/ceramide pathways. These two pathways also serve as a feedback mechanism to inhibit *CYP8B1* gene transcription to maintain hepatic lipid homeostasis (Fig. 7). Increasing Cyp8b1 expression, such as in fasting, diabetes, and NASH, may contribute to dyslipidemia. TCA and DCA are major bile acids; increasing these two bile acids by Ad-Cyp8b1 in this study is relevant to humans.

Our current study is consistent with recent reports that deletion of the *Cyp8b1* gene protects against NASH in mice[14,15], reduces dietary cholesterol absorption from the intestine, prevents hypercholesterolemia and gallstone formation in diabetic mice[40], and prevents atherosclerosis in *Apoe* knockout mice[41]. Ablation of Cyp8b1 also improved glucose homeostasis by increasing GLP-1 secretion[42]. Overall, this current study has identified a novel Cyp8b1/ceramide/mTORC1/SREBP-1c signaling pathway that is modulated by FGF15 and FGF21. These mechanisms may be responsible for dyslipidemia and insulin resistance, and diet-induced obesity. Targeting Cyp8b1 to modulate bile acid composition and mTORC1 signaling may be a potential drug therapy to treat NAFLD.

ACKNOWLEDGMENTS: This study was supported by NIH grants DK44442 and DK58379. We thank Drs. Cen Xie and Frank Gonzalez (NCI, NIH) for the analysis of ceramides and bile acid composition. P.P. performed all the experiments and wrote the manuscript, J.Y.L.C. developed the concept, designed the experiments, interpreted the data, and wrote the manuscript. The authors declare no conflicts of interest.

REFERENCES

1. Chiang JY. Bile acids: Regulation of synthesis. J Lipid Res. 2009;50:1955–66.
2. Murphy C, Perini P, Wang J, Bjorkhem I, Eggertsen G, Gafvels M. Cholic acid as key regulator of cholesterol synthesis, intestinal absorption and hepatic storage in mice. Biochim Biophys Acta 2005;1735(3):167–75.
3. Li T, Chiang JY. Bile acid signaling in metabolic disease and drug therapy. Pharmacol Rev. 2014;66(4):948–83.
4. Wahlstrom A, Sayin SI, Marshall HU, Backhed F. Intestinal crosstalk between bile acids and microbiota and its impact on host metabolism. Cell Metab. 2016;24(1):41–50.
5. Makishima M, Okamoto AY, Repa JJ, Tu H, Learned RM, Luk A, Hull MV, Lustig KD, Mangelsdorf DJ, Shan B. Identification of a nuclear receptor for bile acids. Science 1999;284:1362–5.
6. Keitel V, Haussinger D. Role of TGR5 (GPBAR1) in liver disease. Semin Liver Dis. 2018;38(4):333–9.
7. Maruyama T, Miyamoto Y, Nakamura T, Tamai Y, Okada H, Sugiyama E, Itadani H, Tanaka K. Identification of membrane-type receptor for bile acids (M-BAR). Biochem Biophys Res Commun. 2002;298(5):714–9.
8. Zhang M, Chiang JY. Transcriptional regulation of the human sterol 12a-hydroxylase gene (CYP8B1): Roles of hepatocyte nuclear factor 4a (HNF4a) in mediating bile acid repression. J Biol Chem. 2001;276:41690–9.
9. Pathak P, Li T, Chiang JY. Retinoic acid-related orphan receptor alpha regulates diurnal rhythm and fasting induction of sterol 12alpha-hydroxylase in bile acid synthesis. J Biol Chem. 2013;288(52):37154–65.
10. Arab JP, Karpen SJ, Dawson PA, Arrese M, Trauner M. Bile acids and nonalcoholic fatty liver disease: Molecular insights and therapeutic perspectives. Hepatology 2017;65(1):350–62.
11. Haeusler RA, Astiarraga B, Camastra S, Accili D, Ferrannini E. Human insulin resistance is associated with increased plasma levels of 12alpha-hydroxylated bile acids. Diabetes 2013;62(12):4184–91.
12. Puri P, Daita K, Joyce A, Mirshahi F, Santhekadur PK, Cazanave S, Luketic VA, Siddiqui MS, Boyett S, Min HK, et al. The presence and severity of nonalcoholic steatohepatitis is associated with specific changes in circulating bile acids. Hepatology 2018;67:534–48.
13. Um SH, D'Alessio D, Thomas G. Nutrient overload, insulin resistance, and ribosomal protein S6 kinase 1, S6K1. Cell Metab. 2006;3(6):393–402.
14. Patankar JV, Wong CK, Morampudi V, Gibson WT, Vallance B, Ioannou GN, Hayden MR. Genetic ablation of Cyp8b1 preserves host metabolic function by repressing steatohepatitis and altering gut microbiota composition. Am J Physiol Endocrinol Metab. 2018;314(5):E418–32.
15. Chevre R, Trigueros-Motos L, Castano D, Chua T, Corliano M, Patankar JV, Sng L, Sim L, Juin TL, Carissimo G, et al. Therapeutic modulation of the bile acid pool by Cyp8b1 knockdown protects against nonalcoholic fatty liver disease in mice. FASEB J. 2018;32(7):3792–802.

16. Pathak P, Liu H, Boehme S, Xie C, Krausz KW, Gonzalez F, Chiang JYL. Farnesoid X receptor induces Takeda G-protein receptor 5 crosstalk to regulate bile acid synthesis and hepatic metabolism. J Biol Chem. 2017;292(26):11055–69.
17. Pathak P, Cen X, Nichols RG, Ferrell JM, Boehme S, Krausz KW, Patterson AD, Gonzalez FJ, Chiang JYL. Intestine farnesoid X receptor agonist and the gut microbiota activate G-protein bile acid receptor-1 signaling to improve metabolism. Hepatology 2018;68:1574–88.
18. Xie C, Jiang C, Shi J, Gao X, Sun D, Sun L, Wang T, Takahashi S, Anitha M, Krausz KW and others. An intestinal farnesoid X receptor-ceramide signaling axis modulates hepatic gluconeogenesis in mice. Diabetes 2017;66(3):613–26.
19. Nie B, Park HM, Kazantzis M, Lin M, Henkin A, Ng S, Song S, Chen Y, Tran H, Lai R, et al. Specific bile acids inhibit hepatic fatty acid uptake in mice. Hepatology 2012;56(4):1300–10.
20. Zhou Y, Yu S, Cai C, Zhong L, Yu H, Shen W. LXRa participates in the mTOR/S6K1/SREBP-1c signaling pathway during sodium palmitate-induced lipogenesis in HepG2 cells. Nutr Metab. (Lond) 2018;15:31.
21. Angela M, Endo Y, Asou HK, Yamamoto T, Tumes DJ, Tokuyama H, Yokote K, Nakayama T. Fatty acid metabolic reprogramming via mTOR-mediated inductions of PPAR gamma directs early activation of T cells. Nat. Commun. 2016;7:13683.
22. Bechmann LP, Hannivoort RA, Gerken G, Hotamisligil GS, Trauner M, Canbay A. The interaction of hepatic lipid and glucose metabolism in liver diseases. J Hepatol. 2012;56(4):952–64.
23. Veilleux A, Houde VP, Bellmann K, Marette A. Chronic inhibition of the mTORC1/S6K1 pathway increases insulin-induced PI3K activity but inhibits Akt2 and glucose transport stimulation in 3T3-L1 adipocytes. Mol Endocrinol. 2010;24(4):766–78.
24. Chimin P, Andrade ML, Belchior T, Paschoal VA, Magdalon J, Yamashita AS, Castro E, Castoldi A, Chaves-Filho AB, Yoshinaga MY and others. Adipocyte mTORC1 deficiency promotes adipose tissue inflammation and NLRP3 inflammasome activation via oxidative stress and de novo ceramide synthesis. J Lipid Res. 2017;58(9):1797–807.
25. Owen JL, Zhang Y, Bae SH, Farooqi MS, Liang G, Hammer RE, Goldstein JL, Brown MS. Insulin stimulation of SREBP-1c processing in transgenic rat hepatocytes requires p70 S6-kinase. Proc Natl Acad Sci USA 2012;109(40):16184–9.
26. Bae EJ, Xu J, Oh DY, Bandyopadhyay G, Lagakos WS, Keshwani M, Olefsky JM. Liver-specific p70 S6 kinase depletion protects against hepatic steatosis and systemic insulin resistance. J Biol Chem. 2012;287(22):18769–80.
27. Inagaki T, Dutchak P, Zhao G, Ding X, Gautron L, Parameswara V, Li Y, Goetz R, Mohammadi M, Esser V, et al. Endocrine regulation of the fasting response by PPARalpha-mediated induction of fibroblast growth factor 21. Cell Metab. 2007;5(6):415–25.
28. Potthoff MJ, Inagaki T, Satapati S, Ding X, He T, Goetz R, Mohammadi M, Finck BN, Mangelsdorf DJ, Kliewer SA and others. FGF21 induces PGC-1alpha and regulates carbohydrate and fatty acid metabolism during the adaptive starvation response. Proc Natl Acad Sci USA 2009;106(26):10853–8.
29. Schlein C, Talukdar S, Heine M, Fischer AW, Krott LM, Nilsson SK, Brenner MB, Heeren J, Scheja L. FGF21 lowers plasma triglycerides by accelerating lipoprotein catabolism in white and brown adipose tissues. Cell Metab. 2016;23(3):441–53.
30. Holland WL, Adams AC, Brozinick JT, Bui HH, Miyauchi Y, Kusminski CM, Bauer SM, Wade M, Singhal E, Cheng CC, et al. An FGF21-adiponectin-ceramide axis controls energy expenditure and insulin action in mice. Cell Metab. 2013;17(5):790–7.
31. Marrapodi M, Chiang JY. Peroxisome proliferator-activated receptor alpha (PPARalpha) and agonist inhibit cholesterol 7alpha-hydroxylase gene (CYP7A1) transcription. J Lipid Res. 2000;41(4):514–20.
32. Gong Q, Hu Z, Zhang F, Cui A, Chen X, Jiang H, Gao J, Chen X, Han Y, Liang Q, et al. Fibroblast growth factor 21 improves hepatic insulin sensitivity by inhibiting mammalian target of rapamycin complex 1 in mice. Hepatology 2016;64(2):425–38.
33. Xu J, Lloyd DJ, Hale C, Stanislaus S, Chen M, Sivits G, Vonderfecht S, Hecht R, Li YS, Lindberg RA, et al. Fibroblast growth factor 21 reverses hepatic steatosis, increases energy expenditure, and improves insulin sensitivity in diet-induced obese mice. Diabetes 2009; 58(1):250–9.
34. Gonzalez FJ, Jiang C, Patterson AD. An intestinal microbiota-farnesoid X receptor axis modulates metabolic disease. Gastroenterology 2016;151(5):845–59.
35. Pagadala M, Kasumov T, McCullough AJ, Zein NN, Kirwan JP. Role of ceramides in nonalcoholic fatty liver disease. Trends Endocrinol Metab. 2012;23(8): 365–71.
36. Devkota S, Wang Y, Musch MW, Leone V, Fehlner-Peach H, Nadimpalli A, Antonopoulos DA, Jabri B, Chang EB. Dietary-fat-induced taurocholic acid promotes pathobiont expansion and colitis in Il10−/− mice. Nature 2012; 487(7405):104–8.
37. Wang L, Gout I, Proud CG. Cross-talk between the ERK and p70 S6 kinase (S6K) signaling pathways. MEK-dependent activation of S6K2 in cardiomyocytes. J Biol Chem. 2001;276(35):32670–7.
38. Wan ZY, Tian JS, Tan HW, Chow AL, Sim AY, Ban KH, Long YC. Mechanistic target of rapamycin complex 1 is an essential mediator of metabolic and mitogenic effects of fibroblast growth factor 19 in hepatoma cells. Hepatology 2016;64(4):1289–301.
39. Song KH, Li T, Owsley E, Strom S, Chiang JY. Bile acids activate fibroblast growth factor 19 signaling in human hepatocytes to inhibit cholesterol 7alpha-hydroxylase gene expression. Hepatology 2009;49(1):297–305.
40. Li-Hawkins J, Gafvels M, Olin M, Lund EG, Andersson U, Schuster G, Bjorkhem I, Russell DW, Eggertsen G. Cholic acid mediates negative feedback regulation of bile acid synthesis in mice. J Clin Invest. 2002;110(8): 1191–200.
41. Slatis K, Gafvels M, Kannisto K, Ovchinnikova O, Paulsson-Berne G, Parini P, Jiang ZY, Eggertsen G. Abolished synthesis of cholic acid reduces atherosclerotic development in apolipoprotein E knockout mice. J Lipid Res. 2010;51(11):3289–98.
42. Kaur A, Patankar JV, de Haan W, Ruddle P, Wijesekara N, Groen AK, Verchere CB, Singaraja RR, Hayden MR. Loss of Cyp8b1 improves glucose homeostasis by increasing GLP-1. Diabetes 2015;64(4):1168–79.